# University of Huddersfield Repository

Lane, M., Ashari, Djoni, Ball, Andrew and Gu, Fengshou

Investigation of Motor Supply Signature Analysis to Detect Motor Resistance Imbalances

## Original Citation

# Investigation of Motor Supply Signature Analysis to Detect Motor Resistance Imbalances

M. Lane    D. Ashari    F. Gu   A.D. Ball

Centre for Efficiency and Performance Engineering

University of Huddersfield

Huddersfield, UK

mark.lane@hud.ac.uk

*Abstract*— **The trend to use inverter drives in industry is well established. It is desirable to monitor the condition of the motor/drive combination with the minimum of system intervention and at the same time retaining compatibility with the latest generation of AC PWM vector drives. This paper studies the effect of stator resistance asymmetry on the performance of the motor driven by a latest-generation unmodified AC PWM drive under varying speed conditions. The asymmetry of increased resistance in one phase is intended to simulate the onset of a failing connection between drive and motor but one that is non-critical and will remain undetected in use because the resistance increase is small and does not appear to affect the motor operation significantly. The performance is compared against baseline motor data for the resistance increase. Moreover, it is also examined following an auto-tune on the drive with the asymmetric motor in order to observe if any effects of resistance imbalance can be shown on the sensorless vector control algorithms. Initial results from the motor tests clearly show a difference in values measured from the motor current and voltage signals, which can be a useful indication of the asymmetry of the drive system. t**

*Keywords— Efficiency, Unbalanced, Stator resistance increase, MCSA, PWM, Random switching pattern,Supply Harmonics.*

## I. INTRODUCTION

Motor efficiency in industrial applications is becoming more critical but some traditional motor condition monitoring techniques have been limited to constant speed applications. This series of tests simulates the motor operation over a range of speeds and with a small resistance increase in the motor stator windings that would not normally cause faults to be detected in the inverter drive system itself but could lead to a reduction in motor efficiency and unbalanced running of the inverter drive system that may result in premature failure of the motor and the drive system.

Existing research in this area has covered standard inverter drives without sensorless vector control operation and random-pattern PWM techniques.

The purpose of this research is to determine if the resistance increases can be detected for a motor that is running at variable speeds and also the effect that a motor auto-tune has on performance following a resistance increase.

Although stator resistance increases are not the only cause of motor failures, the nature of the fault is such that it can remain undetected for an extended period of time because once a motor system is installed and commissioned, the drive system is unlikely to be checked for correct operation until the system has failed completely. For companies interested in maintaining the efficiency of plant and equipment there are more favoured non-intrusive methods to be used, such as external vibration measurements to monitor bearings, or thermal imaging techniques for overload monitoring. It is unlikely that electrical checks on motor stator resistances will be carried out due to the equipment having to be brought off-line, the requirement to disturb the motor connections, risk of electric shock in isolating connections and the potential of a future consequential failure of plant equipment attributable to intervention.

Bin Lu et al. [1] recorded that more than 92% of North American paper mills use periodic vibration measurement techniques and reported an increasing take up of MCSA methods in industry. A. Bellini et. al [2] reported on the study of mechanical failures detected in industrial applications by the use of MCSA, but on non-inverter fed motors. Pedro Vicente et al. [3] have studied a simplified scheme for motor condition monitoring on inverter-driven systems. In particular they were used to detect inter-turn short circuit faults, eccentricity and broken rotor bars. Lucia Frosini et al. [4] investigated external monitoring methods such as stator currents and external flux leakage analysis to detect inter-turn faults. However, it is noted that inter-turn winding insulation failures develop within 30 to 60 seconds before the iron core is melted [1]. At this stage of motor failure, there is probably little that can be done in terms of rectification of the fault from the detection of the inter-turn failure to just before the unit fails catastrophically.

The effects of unbalanced supply voltage feeds to an AC motor are well understood and result in the motor operating efficiency being reduced. The voltage imbalances are documented in the NEMA standards for AC induction motor performance but apply more to non-inverter driven motors.

The purpose of this paper is to focus on detecting gradual failures in an inverter-fed motor system before total failure occurs. With early detection and subsequent intervention to correct the gradual faults, the system can be restored to the installed condition and efficiency thus preserving optimum operation of the equipment.

The effect that faults introduced on the motor have on the sensorless vector control model in the drive are also studied, in particular the effect on speed, motor current and voltage output.

To this end, the research adopts an experimental study based on the latest motor drive technology with manually introduced unbalanced conditions.

## II. TEST FACILITIES AND FAULT SIMULATION

### A. Test Rig

The test rig is designed to have a test driving AC motor and a loading DC motor. The AC motor is a three-phase IM with rated output power of 4 kW at a speed of 1420 RPM (two-pole pairs). The AC motor is driven by a Parker 690 PWM inverter with 3 kHz switching frequency and a carrier frequency selected by a random pattern generator enabled by default. The drive is set to operate in sensorless vector control.

For the research to be valid with future drive systems, it is important that valid test results can be obtained from equipment that utilizes the very latest motor control technology and with these advanced switching techniques enabled.

The DC motor is a shunt-wound design to apply different loading to the AC motor drive system. The speed, load and test duration are all programmable and repeatable. The DC motor regenerates to the mains supply through a four-quadrant two phase DC drive.

### B. Operating conditions

In order to make a reliable comparison, data sets for three different motor operating modes were measured based on a test cycle consisting of four speed steps, each with the same operating data applied. A complete test cycle therefore comprises a total of three steps of 4 speed setpoints run contiguously, making 12 speed setpoints in all.

The test run data detailing test run speeds, duration of test and AC motor loading is given Table I and further illustrated with a diagrammatical representation of the total test cycle shown in Figure 1.

| Step number | Speed RPM | Step duration(s) | Load (% of motor FLC) |
|---|---|---|---|
| 1 | 367.5 | 120 | 100 |
| 2 | 735 | 120 | 100 |
| 3 | 1102.5 | 120 | 100 |
| 4 | 1470 | 120 | 100 |

TABLE I.        TEST CYCLE DATA

All test result plots use the x-axis as the "time domain", with each total period of 4 speeds corresponding to one speed step as shown in Figure 1.
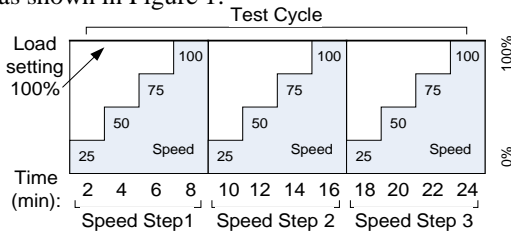


Fig. 1 Test cycle for variable speed test

### C. Fault Simulation

So that tests can be compared between drive operating modes, the drive would be run for each test cycle in the following three modes as follows:

| Drive modes |
|---|
| Healthy motor auto-tuned |
| Motor with simulated faults |
| Motor with simulated faults auto-tuned |

TABLE II.        Drive operating modes

There are a number of phase resistance increments available on the test rig in 0.1Ω steps obtained by changing the wiring tapping on the custom-built resistor unit.

The resistance fault simulated is that which occurs in one winding inside the AC motor thereby affecting only one motor phase. This is indicated in Figure 2, below.
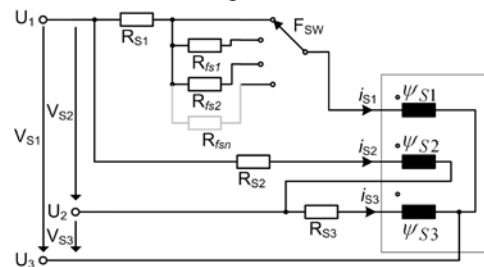


Fig. 2 Motor magnetizing circuit detailing the stator phase resistance fault inserted in one of the three phase connections internally in the motor on phase 1 (DELTA circuit)

### D. Motor winding resistance increments

After a series of baseline healthy tests are run, a stator resistance was applied to the stator winding. This was done in series with the winding and will be referred to as the resistance $R_{fs}$. The effect on the equivalent circuit of the stator is shown in Figure 2 and the effect on one phase resistance increase on the stator equivalent circuit equation is as below:

$$V_{s1} = R_s is+ = \frac{d\psi_{s1}}{dt} \rightarrow V_{s1} = \left(R_{fs} + R_s\right)is+ = \frac{d\psi_{s1}}{dt}$$

This creates an imbalance in the stator circuit and the effect is to reduce the magnetic flux generated by one of the stator windings in proportion to the value of $R_{fs}$. The effect of this is to be studied for motor instability compared to normal running conditions.

It is proposed to use the developed algorithms in MATLAB to indicate differences in the following measurements for the resistance increase.

- Motor voltage, current and speed
- Voltage imbalance of three phases
- Current imbalance of three phase
- Baseline versus fault efficiency comparisons

- Motor Supply Harmonic Signals

## III. MOTOR IMBALANCE SIMULATION TEST RESULTS

This section details and compares the test results obtained from each of the baseline and simulated faulty data sets.

Random pattern PWM switching was enabled for these test results, because this was considered the worst-case condition for trying to extract data from motor current signals due to the random noise floor.

Motor speed is measured from an encoder mounted on the rear of the AC motor. This encoder is purely for speed measurement purposes and is not connected to the inverter drive. The motor encoder resolution is 100 pulses/rev.

### A. Motor Terminal Voltage and Phase Current

Figure 3 presents a plot of motor voltage, current and speed measured at each set motor speed with 100% load applied. It can be seen that over the three phases, no clear voltage difference between testing modes is present when examining over the full speed range.
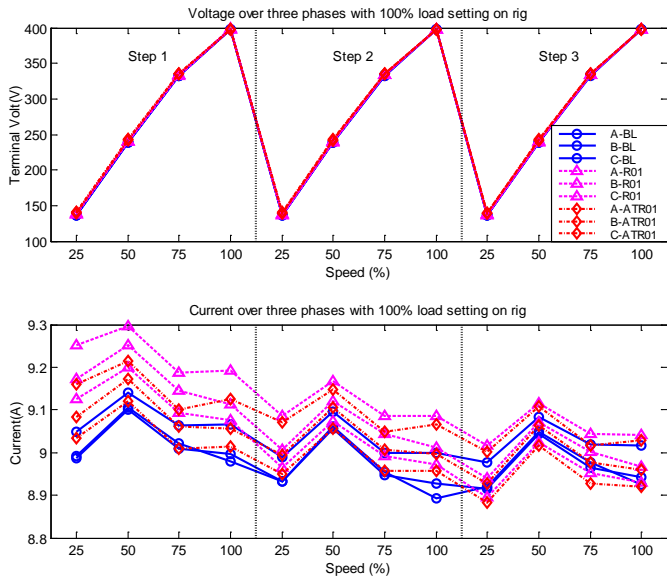
Fig. 3 Plot of voltage over 3 phases: A, B, C, with variable speeds under 100% load setting. BL = Baseline (Healthy Motor); R01 = Stator Resistance of $0.1\Omega$ imbalance; ATR01 = Auto-tune of $0.1\Omega$ imbalance

At a particular speed (50% in Step 1), it can be observed that there was a small difference in motor voltage measured from the baseline data compared to the resistance imbalance and the auto-tuned motor with resistance imbalance but only at the beginning of the tests. Towards the end of the test run, the voltage measurements were seen to be closer to each other, so this set of readings was not very conclusive.

If the current in three phases is observed over the three consecutive test runs, the gradual effect of an increase in motor resistance during the tests is clear as shown in Figure 3, row 2 which presents the data plot for this.

On closer inspection of the motor current signals, an increase in motor stator currents for the resistance increase, and

resistance increase following an auto-tune can be observed at step 1 of the three test runs at a speed of 25%. However, towards the end of the test run at Step 3, the results become inconclusive. At a speed of 50% in step 3 the data from all operating modes are observed to overlap each other.

### B. Motor Current and Voltage Asymmetry

The comparison of motor voltage and current imbalances on each phase gives a more meaningful indication of the actual fault occurring. In Figure 4 it can be seen that there is a marked difference between healthy and induced fault motor voltages (upper graph) and current (lower graph).
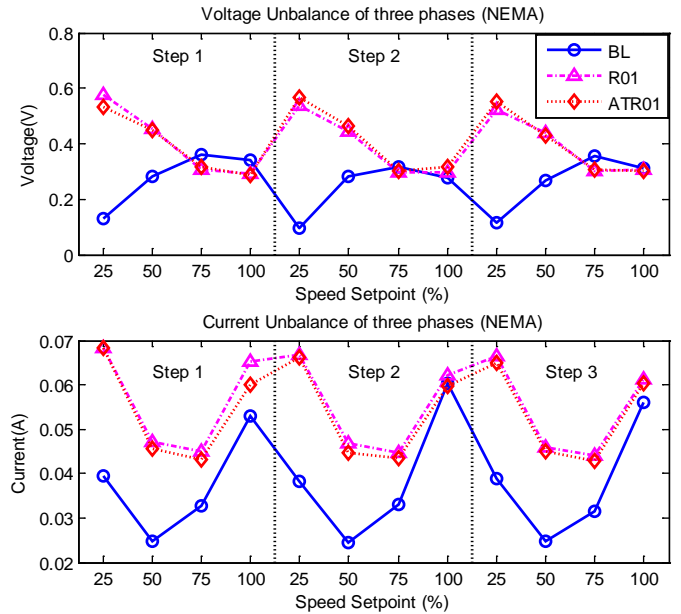
Fig.4 Differences of voltage and currents between three modes

At a motor speed range of 25% to 65%, the voltage unbalance across the motor phases on all three steps showed an increase in motor voltage unbalance. At 65% speed, the unbalanced measurements cross and the baseline motor data indicate more of an unbalance than the faulty and auto-tuned data.

By calculating the difference between motor voltages and currents, the effect that a gradual increase in motor resistance that naturally occurs during the test (due to the increasing motor temperature) has on the displayed test results is reduced and a consistency is restored to the readings. This calculation on the voltage unbalance is in accordance with the NEMA definition under which the Line Voltage Unbalance Rate (LVUR) is defined by:

$$LVUR = \frac{\text{maximum deviation from line voltage}}{\text{average line voltage}}$$

$$LVUR = \frac{\max\left[\left(U_{ab} - U_{lavg}\right), \left(U_{bc} - U_{lavg}\right), \left(U_{ca} - U_{lavg}\right)\right]}{U_{lavg}}$$

Where $U_{ab}$, $U_{bc}$ and $U_{ca}$ are line voltages.

The same method is applied to measure the difference in motor currents using the NEMA definition. The current readings in Figure 4 show that there is a marked difference when the fault resistance is introduced. When an auto-tune is performed on the motor with the resistance fault, the imbalance is still present. This could be explained by the motor model assuming that all three stator resistances are equal, so an auto-tune on an imbalanced motor does not correct for the fault introduced in one phase. This is confirmed by the fact that in the Parker 690 drive, there is only one value for stator resistance, $R_s$ in the motor model. This is studied further in section E, Motor Parameters.

## C. Supply Harmonics

Figure 5 details the current spectrum and supply harmonics present at the maximum motor speed of 1470 RPM.
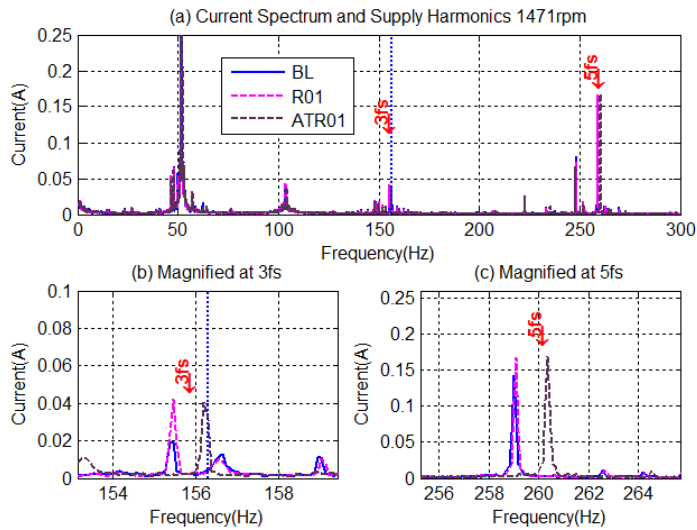


Fig. 5 Current spectrum comparison

Stator asymmetry can change the dynamics of current and voltages. Previous studies [5] show that it increases the amplitudes at higher orders of supply frequency components. Figure 5 presents a comparison of current spectrum between the different operating modes as previously described in Table 2. It shows that the 3rd and 5th harmonics are increased for the two faulty modes at full speed.

Figure 6 details the current and voltage supply harmonics at all speed operating points.

By observing the current measurements, it can be seen that the 3rd harmonic component under imbalanced conditions is consistently increased across all motor speed ranges. The 5th harmonic current component is marginally increased at full speed but the results at 25, 50 and 75% speed do not indicate any difference between the operating modes.

The voltage harmonics do not show any clear difference in either 3rd or 5th harmonic frequencies at any speed and cannot therefore be considered a reliable indicator of stator asymmetry in this case. This could be attributed to the noise generated by the PWM inverter masking out higher harmonic frequencies

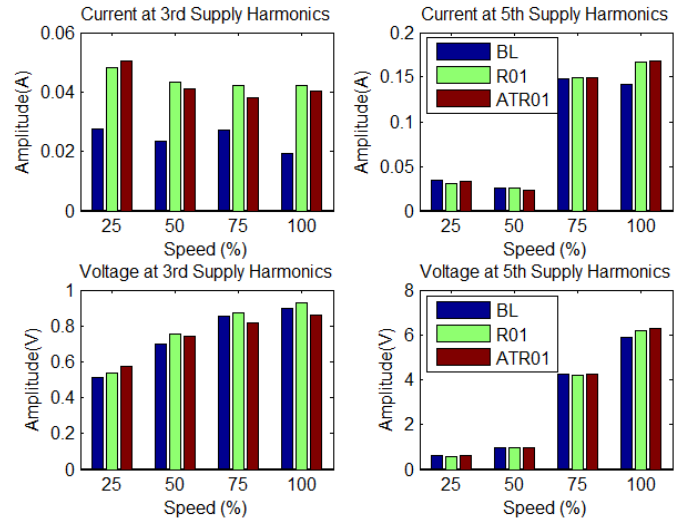especially as the random-pattern PWM generator moves the carrier frequency at random to reduce motor audible noise.



Fig. 6 3rd and 5th harmonic components at different speeds

## D. Efficiency Measurements

The motor power calculations are presented in Figure 7. This shows that the motor input power is increased when the fault resistance is introduced and is further increased when an auto-tune is performed on the faulty motor.
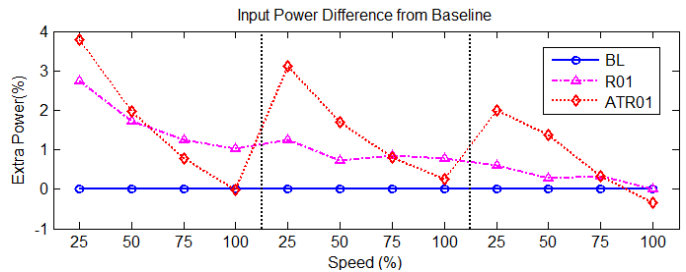


Fig. 7 Motor power calculations

The results clearly show that addition power is consumed by the unbalanced motor at all speeds except at 100% speed. Motor efficiency is reduced at speeds less than the motor rated speed so the difference in additional power required at low speeds is easier to observe. This is not detrimental to the test results because it is often the case that inverters are fitted to motor systems in order to save energy and run at lower speeds thereby allowing the reduced efficiency to be detected in such applications..

## E. Motor Parameters

To observe how the motor model in the sensorless PWM drive is affected by the modification to stator resistance, an auto-tune was performed on the healthy motor, then with the stator resistance of 0.1Ω introduced.

The inverter drive calculates the following values to use in the motor model:

Magnetizing inductance, $L_M$, Leakage Inductance $L_{\sigma S}$, Rotor Resistance $R_R$, Stator resistance $R_S$.

The motor parameters following an auto-tune under healthy conditions and with the fault resistance introduced are shown in Table 3. The data is taken from the Parker SSD ConfigED Lite software package which allows all drive parameters to be loaded on to a computer for analysis.

From Table 3, it can be seen that the increase in stator resistance post-auto-tune calculated by the drive is 0.1658Ω. Auto-tunes 1 and 2 were carried out with the motor at an ambient temperature of 21°C. Auto-tune 3 was carried out after a constant series of test runs that had increased the motor internal temperature to 71°C. The difference in resistance measured was an increase of 0.0695Ω compared to the healthy motor at ambient temperature. This proves that the introduced fault resistance increase of 0.1Ω is more than the resistance increase that would have occurred naturally with the rise in motor temperature.

| Parameter | | AT1 Healthy | AT2 Fault 0.1Ω | AT3 Healthy At 71°C |
|---|---|---|---|---|
| Magnetising current | $I_M$ (A) | 5.16 | 5.09 | 5.15 |
| Stator resistance | Rs (Ω) | 1.1101 | 1.2759 | 1.1796 |
| Leakage inductance | Lσr (mH) | 18.31 | 19.64 | 19.24 |

TABLE III.  AUTO-TUNE DATA (AT)

To observe the effect that the resistance imbalance in one phase has on the drive operating model, it is necessary to study the motor model. During drive operation, the Parker vector drive does not have an adaptive model to compensate for changes in stator resistance during operation. The model is only calculated once by the autotune function. To understand the influence of the motor model on drive operation, a block diagram of a generic IFOC (Inverter Field Oriented Controller) inverter drive is given in Fig. 8 [6].
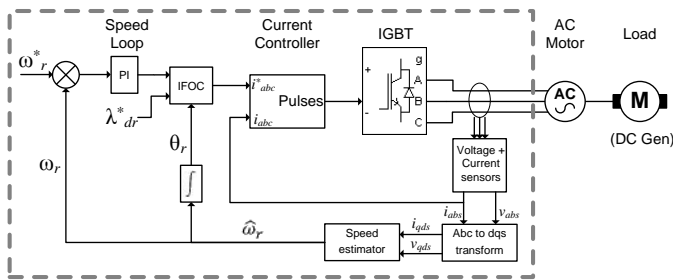
Fig. 8  Inverter FOC diagram

$\omega^*_r$ is the demanded speed, $\lambda^*_{dr}$ the demanded rotor flux. When calculating the current demand output from the IFOC current controller, feedback from the actual motor current and voltage signals are used after transformation from *abc* frame to *dqs* and from there to estimate the rotor angle $\theta_r$. The frequency and voltage output from the inverter are therefore dependent on the rotor speed, predicted by the speed estimator. However, in order for the speed estimator to calculate speed accurately, the motor parameters stored in the drive for the motor model must correspond to the actual motor values.

For sensorless operation, estimated rotor speed $\hat{\omega}_r$ is calculated from the stator current and voltages based on the steady state equivalent circuit of an induction motor [7] as shown in Figure 9.

$$\hat{\omega}_r = \frac{E}{\lambda^{rf}_{dr}} - \frac{R_r}{L_r} \bullet \frac{L_m \bullet i^{rf}_{qs}}{\lambda^{rf}_{dr}}$$

Where E, the air gap voltage can be calculated as follows, based on the rotor stator resistance and inductance.

$$E = V_{qds} - R_s \bullet i_{qds} - \frac{d}{dt} \bullet L_{is} \bullet i_{qds}$$

If the air gap voltage value is incorrect because the stator resistance $R_s$ stored by the motor model in the drive is in error then speed $\theta$ estimated by the drive will also be in error. This manifests itself in the increased voltage and current output from the drive. Even following an auto-tune on the fault, the drive cannot correct for a single phase imbalance. The auto-tune model has not been developed to take account of this fault scenario.
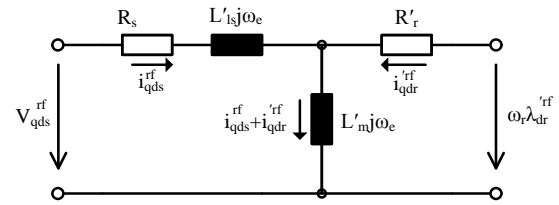
Fig. 9  Induction motor steady state equivalent circuit

## IV. CONCLUSIONS

Initial results from the motor tests clearly show a difference in the motor voltage and current asymmetry values measured and post-processed under MATLAB.

The asymmetry values are more apparent when the motor is more lightly loaded and is running less efficiently.

These initial results are positive, indicating that imbalances in a single stator resistance phase can be observed without the need for spectral analysis of the motor current signals. A motor speed variation was noted under imbalanced conditions, but as an external encoder was used to take these measurement, the results were not documented. This is because the detection methods used for measuring imbalances in this paper should be non-intrusive.

The supply current harmonic measurements show positive results that correspond to existing research on motors driven directly from a clean 3-phase supply. It is important to be able to advance this research on direct-on-line driven motor systems onto inverter-driven systems because of their widespread use.

The test results also provide an insight into the most likely control algorithm used by the Parker 690 drive, which is assumed to be a stator model.

## REFERENCES

[1]  Bin Lu, David B. Durocher, Peter Stemper (2008) Online And Nonintrusive Continuous Motor Energy And Condition Monitoring In

Process Industries. Pulp and Paper Industry Technical Conference, 2008. PPIC 2008. Conference Record of 2008 54th Annual

[2] Bellini, A; Filippetti, F; Franceschini, G; Tassoni, C; Passaglia, R; Saottini, M; Giovannini, M (2003) Mechanical failures detection by means of induction machine current analysis: a case history. 4th IEEE International Symposium on Diagnostics for Electric Machines, Power Electronics and Drives

[3] Pedro Vicente, Jover Rodrı´guez, Marian Negrea, Antero Arkkio (2007) A simplified scheme for induction motor condition monitoring. Laboratory of Electromechanics, Department of Electrical and Communication Engineering, Finland.

[4] Austin HB (1999) The impact that voltage and frequency variations have on AC induction motor performance and life in accordance with NEMA MG-1 standards. In: Conference record of 1999 annual pulp and paper industry technical conference

[5] G. Joksimovic and J. Penman, "The detection of inter-turn short circuits in the stator windings of operating motors," *IEEE Trans. Ind. Electron.*,vol. 47, no. 5, pp. 1078–1084, Oct. 2000.-3fs

[6] Mohamed S. Zaky (2012) Stability Analysis of Speed and Stator Resistance Estimators for Sensorless Induction Motor Drives. IEEE Transactions On Industrial Electronics, Vol. 59, No. 2, February 2012

[7] Joachim Holtz, (2002) Sensorless Control of Induction Motor Drives. Proceedings Of The IEEE, Vol. 90, No. 8, August 2002.